Environmental Technology & Innovation 40 (2025) 104617

Contents lists available at ScienceDirect

Environmental Technology & Innovation

journal homepage: www.elsevier.com/locate/eti

Assessing the environmental sustainability of decentralized photocatalytic treatment in healthcare facilities

Sofía Estévez *, Jorge González-Rodríguez, Isabella Narváez-Prado, Gumersindo Feijoo, María Teresa Moreira

CRETUS, Department of Chemical Engineering, Universidade de Santiago de Compostela, Santiago de Compostela 15782, Spain

ARTICLE INFO

Keywords:
Life Cycle Assessment
Heterogeneous photocatalysis
Wastewater treatment
Pharmaceuticals
Micropollutants

ABSTRACT

The rapid increase in pharmaceutical pollutants in aquatic ecosystems has driven the need for innovative wastewater treatment solutions. This study evaluates the environmental performance of a Fe_3O_4/ZnO nanocomposite-based photocatalytic reactor, applied as a tertiary treatment for hospital wastewater. Life cycle assessment was used to compare four operational scenarios of the photocatalytic reactor, varying oxidant concentration and light intensity. The results show that the reactor is able to achieve 80 % removal efficiency for a complex wastewater mixture of nine micropollutants, meeting the standards outlined in the European legislation. However, compliance with legislation for some highly recalcitrant pollutants (e.g., trimethoprim) may require an increase in equipment size and operation time, resulting in a higher climate change impact (4.94 kg CO_2/m^3) if compared to other compounds that could be used as reference (e.g., 0.37–3.02 kg CO_2/m^3 for diclofenac and 17α-ethynylestradiol, respectively). Since most of the environmental impact of technology comes from the use of electricity in the lamps (65 % of the impact profile), strategies should be developed to offset this high resource demand. Ideally, the solutions should result in an environmental trade-off for freshwater ecotoxicity with lower impacts than direct discharge (3.6 CTUe/m^3). While the variability between scenarios is in the range of 1.07–10.94 CTUe/m^3, the most preferable option resulted in impacts in ecotoxicity of 2.79 CTUe/m^3 and greenhouse gas emissions of 1.20 kg CO_2eq./m^3. This scenario not only resulted in lower direct and indirect environmental impacts on aquatic ecosystems compared to the case where no treatment was applied, but it also nearly fulfilled legislative requirements and remained competitive with other existing technologies such as solar-powered photocatalysis, photo-Fenton, electro-Fenton, and adsorption.

1. Introduction

The rapid increase in the global population has driven exponential industrialization, urbanization, overexploitation of natural resources, and escalating levels of pollution (Mwizerwa et al., 2024). Environmental pollution is largely dependent on the intrinsic properties of pollutants, particularly those influencing their bioavailability, persistence, and bioaccumulation in ecosystems (Kayode-Afolayan et al., 2022). Pollutants of major concern include heavy metals (Mitra et al., 2022; Wei et al., 2025), Persistent Organic Pollutants (POPs) such as polychlorinated biphenyls (Vallero, 2023), dioxins, and pesticides, hydrophobic organic compounds

* Corresponding author.
E-mail address: sofia.estevez.rivadulla@usc.es (S. Estévez).

https://doi.org/10.1016/j.eti.2025.104617
Received 10 July 2025; Received in revised form 7 October 2025; Accepted 8 November 2025
Available online 10 November 2025

Nomenclature

AC	Acidification
AOPs	Advanced Oxidation Processes
CC	Climate Change
CFC	Chlorofluorocarbon
BOD	Biological Oxygen Demand
COD	Chemical Oxygen Demand
DCB	1,2-Dichorobenzene
DCF	Diclofenac
DOC	Dissolved Organic Carbon
CPF	Ciprofloxacin
E1	Estrone
E2	Estradiol
EE2	17α-ethynylestradiol
FE	Freshwater Eutrophication
FET	Freshwater Ecotoxicity
FRU	Fossil Resource Use
HTC	Human Toxicity Cancer
HTNC	Human Toxicity Non-Cancer
IBP	Ibuprofen
IR	Ionizing Radiation
LCA	Life Cycle Assessment
LCI	Life Cycle Inventory
LU	Land Use
MBR	Membrane Bioreactor
ME	Marine Eutrophication
MRU	Mineral Resource Use
NMVOC	Non methane volatile organic compound
NPX	Naproxen
OD	Ozone Depletion
PM	Particulate Matter
POF	Photochemical Ozone Formation
POPs	Persistent Organic Pollutants
PPCPs	Pharmaceutical and Personal Care Products
SMX	Sulfamethoxazole
TE	Terrestrial Eutrophication
TMP	Trimethoprim
TN	Total Nitrogen
TOC	Total Organic Carbon
TP	Total Phosphorus
TSS	Total Suspended Solids
UV	Ultraviolet
WU	Water Use

(Blum et al., 2018), microplastics (Chen et al., 2023), nanoplastics (Menéndez-Pedriza and Jaumot, 2020), and pharmaceuticals, including antibiotics, hormones, and anti-inflammatory drugs (Zenker et al., 2014).

The problem of pharmaceutical contamination stands out as a global concern due to its far-reaching implications. Key concerns include the emergence of antimicrobial resistance (Salam et al., 2023), insufficient international regulation on environmental risks (Miettinen and Khan, 2022), and rising pharmaceutical consumption linked to demographic trends. Current consumption of pharmaceuticals exceeds 100,000 tons per year, and the global market is expected to grow by approximately 6 % per year between 2023 and 2030 (Grand View Research, 2025).

Pharmaceuticals and their metabolites frequently enter wastewater systems through domestic, agricultural and industrial sources, eventually reaching aquatic ecosystems (Gaw et al., 2014). Over 600 pharmaceuticals are detectable at significant concentrations, with the most prevalent being antibiotics (e.g., sulfamethoxazole, trimethoprim, ciprofloxacin), anti-inflammatory drugs (e.g., diclofenac, ibuprofen, naproxen), and hormones (e.g., estradiol, 17α-ethynylestradiol, and estrone) (aus der Beek et al., 2016; Manickum and John, 2014). Among them, 477 different pharmaceutical compounds have been detected in European water bodies, accounting for 92 % of toxic micropollutants in European wastewater (An et al., 2024; European Council, 2024). These substances pose significant risks to aquatic and terrestrial wildlife, as well as to human health, due to their biologically active and recalcitrant nature, rendering

them resistant to conventional degradation processes (El-Fawal et al., 2020).

Conventional wastewater treatment methods, such as coagulation, flocculation, sedimentation and filtration, typically remove less than 25 % of Pharmaceutical and Personal Care Products (PPCPs) (Archer et al., 2017). Biodegradation processes, particularly for recalcitrant PPCPs, have shown limited effectiveness. To mitigate the environmental impact of PPCP discharge, advanced water treatment technologies have been developed, such as membrane filtration, adsorption (e.g., using activated carbon or graphene oxides), advanced oxidation processes (AOPs) and ultrasonication (Krishnan et al., 2021). However, adsorption and filtration merely transfer PPCPs from water to solid phases, neither degradation nor detoxification of contaminants is achieved (Ghazal et al., 2022). In contrast, AOPs show promise for the mineralization of recalcitrant micropollutants into carbon dioxide and water (Tufail et al., 2020).

Among AOPs, alternatives such as Fenton-based processes, ozonation, electrochemical oxidation, photocatalysis and photolysis stand out (Merchant et al., 2024). The conventional Fenton process, a well-established AOP, efficiently removes organic pollutants from wastewater by utilizing hydrogen peroxide (H_2O_2) as oxidizing agent and ferrous ions (Fe^{2+}) as catalysts. It is most effective within a narrow pH range (typically below 3), generates red sludge and involves substantial economic costs in large-scale applications (Wang et al., 2016). In addition to Fenton oxidation, other systems have been investigated, such as peroxydisulfate- or peroxymonosulfate-based AOPs. However, these systems can produce high concentrations of sulfate ions (SO_4^{2-}), which may be reduced to hydrogen sulfide or, in the presence of ammonium, lead to the formation of nitrophenolic compounds. Both of them can disrupt microbial activity (Ma et al., 2022). On the other hand, photocatalysis using semiconductors has gained attention due to its ability to degrade organic pollutants by generating reactive oxygen species. This technique overcomes the limitations of other methods, such as high pH requirements or the generation of secondary contaminants. However, photocatalysis requires external energy sources for light activation and the use of specific catalysts (Zhong et al., 2021).

On the other hand, advanced oxidation processes based on heterogeneous catalysts with semiconducting properties emerged in recent decades as an alternative to conventional homogeneous technologies, since these materials provide high stability in solution, biological and chemical inertness, and can be customized with doping agents to improve their photocatalytic properties. Apart from this, they can be reused for a long time through the implementation of adequate separation steps or immobilization techniques, such as filtration or immobilization on fibers, spheres or carriers (Ibhadon and Fitzpatrick, 2013). However, there are limitations for their use, including charge recombination, mass transfer restrictions as well as higher costs compared to previously reported AOPs (Iervolino et al., 2020). Likewise, the catalyst manufacturing processes are complex, and their recovery may limit their potential for widespread application due to environmental and cost-related concerns (Pavlović et al., 2024). One possible solution is the use of nanostructured magnetite (Fe_3O_4), which offers superparamagnetic properties that facilitate easier isolation and reuse from wastewater through an external magnetic separation system (Elshypany et al., 2021). This approach improves the sustainability of the photocatalytic process by enabling catalyst reuse and reducing synthesis-related impacts. However, to ensure that these new catalysts do not inadvertently worsen process conditions or create unintended environmental impacts, comprehensive environmental studies should be conducted during the early design stages. Such studies will inform decisions regarding both the design and operation of the process, aligning it with sustainability goals.

Life Cycle Assessment (LCA) is a commonly used methodology for evaluating the environmental impacts of processes and technologies. While most LCA studies on photocatalysis focus on titanium dioxide (TiO_2)-based systems (Elhami et al., 2023; Pesqueira et al., 2024), there is limited research on alternative materials like Fe_3O_4/ZnO, especially for complex wastewater streams containing pharmaceutical pollutants (Costamagna et al., 2020).

Furthermore, existing LCAs often target synthetic or single-component wastewaters, which do not accurately represent the composition of real hospital effluents (Foteinis et al., 2018; Pesqueira et al., 2021). Notably, most environmental analyses of photocatalysis omit pharmaceutical wastewater as a target matrix. Some studies have analyzed components such as methylene blue dye (Kong et al., 2023), phenol (Costamagna et al., 2020; Magdy et al., 2021), kraft mill bleaching (Muñoz et al., 2005), α-methyl--phenylglycine (Muñoz et al., 2006), olive mill wastewaters (Chatzisymeon et al., 2013), cyanide (Dubsok et al., 2022), sodium dodecylbenzenesulfonate (Dominguez et al., 2018) and Rhodamine B (Elhami et al., 2023). Among those that have addressed pharmaceuticals, Foteinis et al. (2018) (17α-ethynylestradiol), Giménez et al. (2015) (metoprolol) and Pesqueira et al. (2021), (2024) (carbamazepine, diclofenac and sulfamethoxazole) stand out. The latter two are likely the only studies on pharmaceutical micropollutant removal that involve more than one compound in the influent composition.

From an environmental-technological perspective, various treatment methods have been compared, including heterogeneous photocatalysis (with and without H_2O_2), photo-Fenton, the coupling of photocatalysis with photo-Fenton, solar photolysis (with and without H_2O_2), adsorption by activated carbon, electro-Fenton, wet air oxidation, and electrochemical oxidation over boron-doped diamond electrodes. The outcomes of these studies have been inconsistent. Some research indicates that solar-driven technologies, such as photo-Fenton or photolysis, have a worse environmental profile than photocatalysis (Muñoz et al., 2005; Pesqueira et al., 2021), while other studies suggest the opposite (Giménez et al., 2015; Magdy et al., 2021).

While most studies have focused on laboratory-scale systems, only a limited number have progressed to pilot-scale operation (Wang et al., 2021). However, selecting the appropriate treatment capacity is crucial to adapt laboratory processes for industrial applications, meeting efficiency objective (Crater and Lievense, 2018; Zhang et al., 2025). The reactor performance must take into account several factors, including temperature, pH, light intensity, pressure, oxygen concentration, pollutant composition, photocatalyst concentration, reactor geometry, and the presence of oxidizing agents (Sacco et al., 2020). Larger-scale systems benefit from increased equipment efficiency (e.g., improved electrical performance of centrifugal pumps), leading to reduced energy consumption and environmental impact.

Since pilot-scale technology has already been developed, the next step is to deploy a demo-scale system to meet the practical requirements of full-scale wastewater treatment. Using Fe_3O_4/ZnO as the catalyst, the research evaluates four operational scenarios

with primary data, varying oxidant concentration and light intensity. Additionally, nine hypothetical scenarios were developed for a sensitivity analysis to determine whether achieving the minimum removal threshold imposed by European legislation (80 %) results in a more sustainable strategy than direct effluent discharge. Furthermore, the recovery capacity of the magnetic nanocatalyst was evaluated to identify how changes in this parameter influence the environmental profile. The findings contribute to bridging the gap between laboratory-scale innovations and industrial applications, providing insights into the sustainability of advanced photocatalytic technologies for real-world wastewater treatment challenges.

2. Methodology and methods

2.1. Technology description

Pilot-scale experimental data were obtained from a three-section tertiary treatment system, consisting of an influent wastewater storage (Section 1), a photocatalytic degradation reactor (Section 2), and an effluent storage unit (Section 3), as shown in Fig. 1. The stirred photocatalytic reactor (R-201 in Fig. 1) has a capacity of 75 L and operates in batch mode with approximately 30 % headspace. It consists of a cylindrical vessel with a conical bottom, measuring 0.75 m in height and 0.50 m in diameter. Four 130 W ultraviolet (UV) lamps are positioned equidistantly around the reactor and activated simultaneously during operation.

Due to their internal placement, the UV lamps TUV 55 W HF PL-L (Philips, Netherlands) deliver the UVC radiation directed towards the reactor center. According to the information provided by manufacturer is 1.7 mW_{UVC}/cm^2, that is in line with the data of other works. Additionally, this value is below the value of 20 mW/cm^2 at which the rate of the reaction exhibited a linear relationship with the corresponding rise in light intensity (Iyyappan et al., 2024). On the other hand, the studies of Tra et al. (2023) and Anucha et al. (2021) obtained values similar to ours: 0.28 and 1.2 mW/cm^2, respectively.

The UV light excites the surface of the semiconductor nanoparticles onto which contaminants are adsorbed. The catalysts consist of ZnO of 15 nm size in which the magnetite nanoparticles are deposited following a modified Massart method procedure (Massart, 1981), to improve catalysts separation applying external magnetic fields. The final composite reaches an average size of 690 $\pm$ 134 nm with spherical shape, as seen in Fig. A1 of Supplementary Materials A. The photons emitted by the artificial light initiate redox reactions, leading to the formation of hydroxyl and superoxide anion radicals (Frederichi et al., 2021).

To maintain the nanoparticles suspended in the reactor, the wastewater is continuously agitated and recirculated by a single-phase centrifugal pump (model EBARA CDXM/A 70/07, P-202). Located at the base of the R-201 reactor tank, the pump also prevents light from interacting with the reactor internals by directing the liquid into an annular diffuser at the bottom of the cylindrical vessel. Catalyst loading is a key parameter for effective pollutant removal in photocatalytic processes. An optimal loading of 200 ppm was chosen to enhance the formation of electron-hole pairs and minimize overlap, ensuring that photons reach all layers of the photocatalyst, not just the upper layers (Guerra et al., 2019).

The reactor is emptied using a vane pump (VEVOR model MP-15RM, P-301) with a fixed flow rate of 14 mL/min. The reactor effluent is stored in a buffer tank (TK-301) to adjust pH if necessary. Subsequently, catalytic particles are recovered using a magnetic separator and returned to the reactor by pumping a concentrated solution separated from the effluent. The system also includes a second buffer tank (TK-101) for the influent wastewater, allowing for continuous operation when coupled with other treatment stages. Finally, hydrogen peroxide is added from the TK-201 tank to the R-201 reactor to generate highly reactive hydroxyl radicals in the presence of the photocatalyst, thereby enhancing photocatalytic activity.

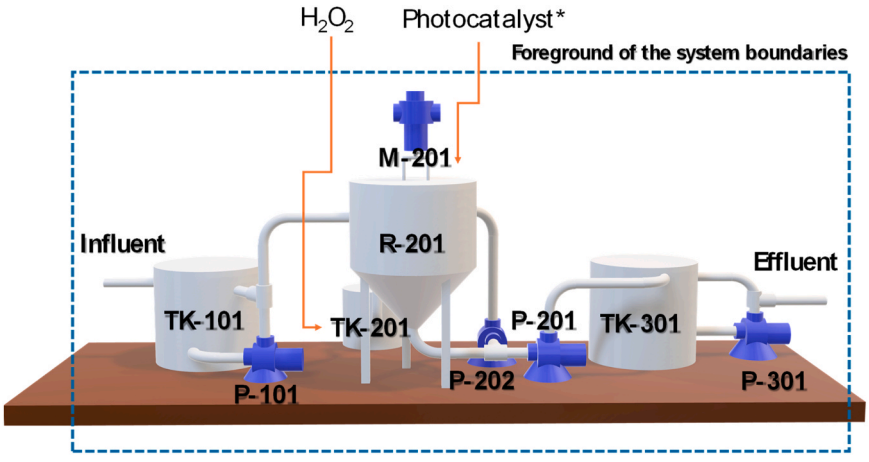

Fig. 1. Process flow diagram (PFD) for photocatalytic micropollutant removal system. Acronyms: TK-101: Influent storage tank; TK-201: Hydrogen hydroxide storage tank; TK-301: Effluent storage tank, R-201: Photocatalytic reactor; P-101: Influent feeding pump; P-201: Reactor effluent pump; P-202: Reactor recycling pump; P-301: Discharge pump; M-201: Motor for magnetic separation.

2.2. Technology goals and reasoning behind the proposal of case studies

To optimize the performance of the pilot-scale reactor described in Section 2.1., a two-level experimental design was implemented. This approach involved varying hydrogen peroxide concentrations and light intensity while maintaining a constant catalyst concentration of 200 ppm, consistent with the typical catalyst loading range of 0.02–1.0 g/L (Ruziwa et al., 2023). This fixed concentration was chosen to optimize reaction rates and light penetration, while minimizing issues such as particle aggregation, which can hinder efficiency and increase environmental impacts from excessive catalyst use. Four operational scenarios were designed to assess reactor performance:

1. **Scenario PL:** 200 mg/L of H_2O_2, 0.972 mW/cm^2 (between 290–390 nm) of light intensity (with 4 UV lamps operative) and pollutant concentrations of 100 μg/L for pharmaceuticals (10 μg/L for hormones).
2. **Scenario PL/2:** Identical H_2O_2 concentration as PL, but with half the light intensity achieved by switching off two UV lamps.
3. **Scenario P/2 L:** Reduced H_2O_2 concentration (100 mg/L) while maintaining the same light intensity as PL.
4. **Scenario L:** Without the addition of H_2O_2 but the same conditions of pollutant concentration and light intensity than PL.

These scenarios were designed to determine the kinetic constants for the targeted pollutants using first-order kinetic equations, and to assess the scalability of the system. The findings have supported the development of mass balance models for various operational systems, including continuous flow systems, aiding the transition from batch to industrial-scale wastewater treatment. The average kinetic constants used for modelling can be found in Table A1.

From the scaled-up data obtained from the pilot-scale experiments, assumptions were taken to consider the photocatalytic reactor as the tertiary treatment of a decentralized system (using membrane bioreactors as the secondary treatment) serving a 200-bed hospital. The treatment capacity was set at 114.5 m^3 /d, based on reported hospital wastewater flow rates, which range from 19 to 2258 L/bed·d (Majumder et al., 2021; Ministerio de Sanidad, 2023). The influent characteristics were based on typical hospital wastewater parameters for the pharmaceuticals. Hospital wastewater typically contains concentrations of anti-inflammatory drugs, antibiotics, and hormones that are 8–15, 5–10, and 1–3 times higher, respectively, than those found in urban wastewater (Verlicchi et al., 2010). Therefore, the average concentrations listed in Table 1 were used for the selected pharmaceuticals in this research.

Several assumptions were considered during the modelling and scale-up:

1. The design is based on a cylindrical photocatalytic reactor operating with the nanocatalyst in suspension in batch mode, without light reflection from the walls.
2. The study focused on the mineralization of the selected micropollutants under light exposure and varying hydrogen peroxide concentrations. Typically, the redox reactions of the species involved occur in multiple stages, generating intermediates. However, secondary reactions between the primary micropollutants and the degradation intermediates were considered negligible. It was also out of scope of this research the analysis of the changes in environmental impacts when considering other pollutants, and their reactions, beyond those of the previously mentioned pharmaceuticals. Therefore, other parameters that may influence in the overall COD or BOD degradation rates were not considered. This strategy prevents double counting in the impacts, since every pollutant has been associated with specific environmental emissions factors based on its chemical structure. Because of this, the impacts results achieved within this research for water eutrophication and ecotoxicity might be modified when incorporating other pollutants.
3. For reactor operation under atmospheric conditions, the effect of temperature was assumed to have no impact on the removal rates. Additionally, at ambient temperatures, external energy for heating was deemed unnecessary.
4. The light intensity near the lamps of the pilot-scale reactor, as monitored during this research, is 0.972 mW/cm^2, which is under the value of 20 mW/cm^2 at which the reaction rate exhibited a linear relationship with the corresponding increase in light intensity (Iyyappan et al., 2024).

Table 1
Composition of hospital wastewaters, average values based on various literature sources expressed in ng/L.

Pollutants	Hernández-Tenorio et al., 2022	Dawood et al., 2023	Khan et al., 2021	Carraro et al., 2016	Carraro et al., 2016	Ajala et al., 2022	Zhao et al., 2021	Average
E1			30			25		27.39
E2			8.0			20.0	30.0	16.87
EE2						35		35.00
IBP	70,544		83,500	2888.5	1453	25,010	7,800	12,998.2
NPX	3,420					10,500	5,600	5,858.70
DCF	1,576			989	285.85	7620	883	1,245.55
SMX		3,000	390	12,716	1057	41,520	9,800	4,308.74
TMP	2,545.5	26,100	330			7,505	7,700	4,174.01
CPF	13,707	4,300				62,515	8,372.9	13,253.11

Note: E1: Estrone; E2: Estradiol; EE2: 17α-ethynylestradiol; IBP: Ibuprofen; NPX: Naproxen; DCF: Diclofenac; SMX: Sulfamethoxazole; TMP: Trimethoprim; CPF: Ciprofloxacin.

5. The system operates isothermally, with micropollutant concentrations below 1 mg/L (Wang et al., 2021). Given the low organic content and solid concentration in the influent wastewater, its properties can be considered similar to those of water in terms of viscosity and density.
6. A 1 % loss of the photocatalyst per batch was assumed. As the nanoparticle does not undergo any change in its chemical structure during the treatment cycles, the catalyst must be replenished up to 200 mg/L to compensate for inefficiencies in the magnetic separation process (González-Rodríguez et al., 2021a). In this regard, the studies of Gamallo et al. (2018) and Fernández et al. (2020) demonstrated the feasibility of reuse of superparamagnetic iron oxide nanoparticles in multiple cycles, being the rate of loss of around 0.07 %–1.38 % and 0.5 %, respectively.

2.3. Life Cycle Assessment

As outlined in previous Section 2.2, the inventory data from pilot-scale experiments were extrapolated to a scaled-up operation to foresee the environmental hotspots of the photocatalytic reactor. This analysis followed the LCA methodology in accordance with ISO 14,040 and 14,044 standards (ISO, 2006). The study adopted a *Cradle-to-grave* approach, covering both the direct and indirect emissions from the operation of the technology. Thus, construction, maintenance and dismantling phases were not analyzed. This system has been characterized by three dimensions of the system boundaries: technological, geographical and temporary. Considering the technological boundaries, our research could not be classified as *gate-to-gate* since we want to incorporate the effect also of indirect emissions. Possible direct emissions for this type of tertiary treatment could be gases from the mineralization of micropollutants (such as CO_2), the parent compounds that remain in the effluent after the treatment, the products of the transformation that are discharged into the waters and the catalysts that are lost (since the recovery systems are not completely efficient). Among these, the parent compound and catalysts discharge effects could be incorporated into this environmental impact assessment, but not that of the transformation of co-products from micropollutants (due to lack of knowledge about the characterization factors). When it comes to the gaseous streams, the IPCC (Intergovernmental Panel on Climate Change) indicates that CO_2 emissions from domestic wastewaters can be considered biogenic (IPCC, 2019). Despite being highly loaded in recalcitrant compounds, hospital effluents are often regarded as domestic and thus discharged into municipal sewers. Besides, the majority of the pollutants originate from human feces, which have been produced in the short-term.

Indirect emissions were incorporated from the background processes of the Ecoinvent® V3.10 database, considering as raw consumables the hydrogen peroxide and electricity. The replacement of photocatalyst material, accounting for losses during magnetic separation recovery, cannot be found the Ecoinvent® database and thus, inventory and environmental impact data related to its consumption were obtained from Feijoo et al. (2017). Apart from these three inputs, the influent wastewater is the last input of the system. However, upstream impacts were not included from the wastewater since the system model of cut-off by ranking for allocation has been selected. This implies that wastewater is a burden-free inflow, as in this model any type of waste is assumed to be the producer's responsibility (in this case the hospital).

When it comes to geographical system boundaries, the photocatalytic treatment was studied within a Spanish/European context (using the Spanish electricity mix, hydrogen production average data for Europe and characterization factors for this region). There were no limitations in the temporary system boundaries since Ecoinvent® data was needed for the background processes and

Table 2
Life Cycle Inventory for the operation of the photocatalytic reactor for the four proposed scaled-up scenarios and functional unit (1 m^3 of wastewater).

Life Cycle Inventory Analysis	PL	PL/2	P/2 L	L
Inputs from Technosphere				
Chemicals				
Hydrogen peroxide (g/m^3)	126.74	126.74	63.37	0.00
Magnetic nanoparticles (replacement only) (mg/m^3)	1.27	1.27	1.27	1.27
Energy				
Pump for mixing tank (kWh/m^3)	0.18	0.18	0.18	0.18
Pump for mixing reactor (kWh/m^3)	0.24	0.24	0.24	0.24
Pump for discharging reactor (kWh/m^3)	$3.48{\cdot}10^{-2}$	$3.48{\cdot}10^{-2}$	$3.48{\cdot}10^{-2}$	$3.48{\cdot}10^{-2}$
Pump for recycling in buffer tank (kWh/m^3)	0.18	0.18	0.18	0.18
Lighting (kWh/m^3)	1.23	0.61	1.23	1.23
Emissions to the environment				
Treated effluent				
Estrone (μg/m^3)	4.24	3.96	4.34	4.50
Estradiol (μg/m^3)	1.29	1.40	1.29	1.50
17α-ethynylestradiol (μg/m^3)	7.01	7.45	7.03	7.99
Ibuprofen (mg/m^3)	0.23	0.29	0.30	0.35
Naproxen (mg/m^3)	0.73	0.95	0.82	1.12
Diclofenac (mg/m^3)	0.07	0.05	0.02	0.03
Sulfamethoxazole (mg/m^3)	0.43	0.49	0.27	0.61
Trimethoprim (mg/m^3)	0.86	0.96	0.93	1.00
Ciprofloxacine (mg/m^3)	0.29	0.46	0.33	0.99
Iron oxide (mg/m^3)	1.27	1.27	1.27	1.27

Notes: PL: 200 mg/L of H_2O_2, 1.12 W/m^2; PL/2: 200 mg/L of H_2O_2, 0.56 W/m^2; P/2 L: 100 mg/L of H_2O_2, 1.12 W/m^2; L: 0 mg/L of H_2O_2, 1.12 W/m^2.

foreground data taken from laboratory experiments can be dated in 2025.

The Life Cycle Inventory (LCI) of the four proposed scenarios is presented in Table 2. The inventory data was processed using the SimaPro 9.6.0.1 software, which translates inputs, outputs, and emissions into environmental impact scores (Pré Sustainability, 2024). An attributional LCA modeling approach was chosen, as it evaluates the environmental impacts of processes or products without considering indirect behavioral consequences (Finnveden and Potting, 2014).

The functional unit (FU) for the study is defined as "the treatment of 1 m^3 of wastewater (Paulu et al., 2021), achieving at least 80 % removal for the reference pollutant of the pharmaceutical wastewater mixture". Sulfamethoxazole was selected as the reference compound for the PL scenario based on the following criteria: (1) it is among the three most concentrated pollutants in the influent, (2) it exhibits one of the three lowest removal efficiencies, and (3) it allows for feasible residence times and reactor volumes. This FU ensures steady-state operation and reflects both volume and micropollutant removal, which are critical for comparing photocatalytic technologies in wastewater treatment.

Table 4 highlights the LCA methodologies considered in the literature. ReCiPe 2016 was used in 7 out of 14 studies listed; however, it lacks characterization factors for most micropollutants analyzed (6 out of 9 in Table 3). To overcome this limitation, alternative methods, such as Impact World + midpoint and EF 3.1, were identified as more suitable for assessing environmental impacts on aquatic ecosystems. These methods offer a comprehensive environmental profile, considering factors like climate change, eutrophication, and resource depletion. USEtox was applied for the toxicity categories. Impact World+ also utilizes USEtox for assessing ecotoxicity and human toxicity, but the parameters have been adjusted at a global level.

Since the treatment facility is located in Spain (Europe), EF 3.1 has been selected as the impact assessment method for this study. This choice is due to the fact that EF 3.1 partially addresses regionalization, with characterization models that are representative of Europe (Bulle et al., 2019). In other words, it assumes that all life cycle emissions and resource consumption occur under European conditions. However, this may not fully reflect the global context, where certain chemicals may be sourced from other regions, and where legislative measures in some countries may not be as stringent as those in Europe. Despite EF 3.1 offering a larger number of characterization factors for toxicity, the SimaPro methods currently lack factors for 17α-ethynylestradiol, naproxen, and ciprofloxacin. As a result, these substances have been assumed to behave similarly to estradiol, ibuprofen (since it is also a propionic acid derivative), and enrofloxacin in the environment.

Based on the midpoint method selected, the impact categories under study are: climate change (CC – kg $CO_{2\ eq.}$), acidification (AC – mol $H^+_{eq.}$), freshwater ecotoxicity (FET - CTU_e), particulate matter (PM – disease inc.), marine eutrophication (ME – kg $N_{eq.}$), freshwater eutrophication (FE – kg $P_{eq.}$), terrestrial eutrophication (TE – mol $N_{eq.}$), human toxicity cancer (HTC - CTU_h), Human toxicity non-cancer (HTNC - CTU_h), ionizing radiation (IR – kBq U-$235_{eq.}$), land use (LU - Pt), ozone depletion (OD – kg $CFC11_{eq.}$), photochemical ozone formation (POF – kg $NMVOC_{eq.}$), fossil resource use (FRU - MJ), mineral resource use (MRU – kg $Sb_{eq.}$) and water use (WU – m^3 deprived). All the cited MidPoint impact categories were chosen for the analysis. The rationale behind this is the anticipated application and future comparison of the results from this LCA study with those of other state-of-the-art studies, as well as the ability to correlate these results with upcoming Product Environmental Footprints conducted under the Commission Recommendation (EU) 2021/2279 of 15 December 2021 on the use of the Environmental Footprint methods to measure and communicate the life cycle environmental performance of products and organizations.

2.4. Proposal for the sensitivity analysis

The selection of the target component within a complex mixture of micropollutants, the energy consumption from the operation of the reactor and the catalyst losses caused by inefficiencies in the permanent magnetic separation unit can be recognized as sensitive parameters in the environmental profile of a photocatalytic wastewater treatment process. The first two critical aspects were withdrawn from the environmental outcomes, taken the analysis of the baseline scenario PL and, thus, can be found in the results section of

Table 3
Availability of characterization factors among impact methods for the selected pharmaceuticals of the study.

Name of pharmaceutical	All SimaPro methods	ReCiPe 2016 V1.08	EF 3.1	Impact World + midpoint V1.02	CML- IA Baseline	Traci 2.1 V1.07
Estrone						
Estradiol						
17α-ethynylestradiol						
Ibuprofen						
Naproxen						
Diclofenac						
Sulfamethoxazole						
Trimetoprim						
Ciprofloxacine						
Total of "yes"	**6**	**3**	**6**	**6**	**0**	**4**

Note: The green color indicates that the characterization is available and the red color that it is not.

Table 4
Characteristics of the life cycle assessment studies found within the literature for photocatalytic treatment of wastewaters.

Catalyst material	Target compound	Functional unit	Software	Method	Reference
Titanium oxide	Kraft mill bleaching wastewater	The removal of 15 % DOC from 1 m^3 kraft pulp mill wastewater	NA	NA	Muñoz et al. (2005)
Titanium oxide	α-methyl-phenylglycine	To treat 1 m^3 of synthetic α-methyl-phenylglycine solution (500 mg/L)	SimaPro 6.0	Institute of Environmental Sciences of Leiden	Muñoz et al. (2006)
Titanium oxide	Olive mill wastewater	1 L of olive mill wastewater	SimaPro 7.3.3	IPCC 2007 V1.02 and ReCiPe V1.06, hierarchist and egalitarian	Chatzisymeon et al. (2013)
Titanium oxide	Metoprolol	The removal of 30–50 % TOC from 1 L of 50 mg/L metropolol aqueous solution	SimaPro 7.0	NA	Giménez et al. (2015)
Titanium oxide	17α-ethynylestradiol	1 μg of 17α-ethynylestradiol from 1 L of wastewater	SimaPro 8.0	ReCiPe 2016 endpoint method, hierarchist	Foteinis et al. (2018)
Titanium oxide Aeroxide® P25	Sodium dodecylbenzenesulfonate	1 m^3 of treated greywater with 90 % reduction of the Sodium dodecylbenzenesulfonate initial concentration	Gabi 6.0	NA	Dominguez et al. (2018)
Zinc oxide doped with rare earth elements	Phenol	The reaction constant to complete degradation of 60 mg/L of phenol in MilliQ water	SimaPro 8.0	Cumulative Energy Demand and the IPCC 2013 GWP 100 y	Costamagna et al. (2020)
Titanium oxide P25	CBZ, DCF, SMX	The treatment of 1 m^3 of urban secondary wastewater containing 5 μg/L of CBZ, DCF and SMX	SimaPro 9	ReCiPe 2016 midpoint method and USEtox	Pesqueira et al. (2021)
Activated carbon/ titanium oxide	Phenol	1 m^3 of phenol solution with an initial concentration of 100 mg/L	SimaPro	CML 2000 baseline method and Eco-indicator 99 method	Magdy et al. (2021)
Titanium dioxide/ iron (III) chloride	Cyanate and cyanide	The degradation of 98 % cyanate from 1 L wastewater	SimaPro 9.0	IMPACT 2002+ method	Dubsok et al. (2022)
Graphene oxide/ titanium oxide	Methylene blue	1 kg TiO_2/rGO	Gabi	ReCiPe 2016 V1.1 midpoint and endpoint method, hierarchist	Kong et al. (2023)
Chlorophyll/ titanium oxide	Rhodamine B	The degradation of 1 kg rhodamine B	SimaPro 9.0.0.48	ReCiPe 2016 V1.03 midpoint and endpoint method	Elhami et al. (2023)
Titanium oxide	Greywater	1 m^3 of water for toilet flushing	NA	ReCiPe 2016 midpoint method, hierarchist	de de Simone Souza et al., (2023)
Graphene oxide/ titanium oxide	CBZ	The treatment of 1 m^3 of urban secondary wastewater to remove 5 μg/L of CBZ	SimaPro 9.4.0.2	ReCiPe 2016 midpoint	Pesqueira et al. (2024)

Notes: CBZ: Carbamazepine; DCF: Diclofenac; DOC: Dissolved Organic Carbon; NA: Not Available; TOC: Total Organic Carbon; SMX: Sulfamethoxazole.

this manuscript. The last assumption was taken from other results from literature beyond that of Gamallo et al., (2019) and Fernández et al. (2020). In this regard, González-Rodríguez et al., (2021b) demonstrated that the recovery rate of the could vary between around 28 %-86 % depending on whether the separation is performed for bare, polyacrylic acid coated or supported nanoparticles. This is indicative that the catalyst losses may be dependent on a multitude of aspects including magnetic properties, size, zeta potential, agglomeration or matrix composition.

Therefore, the first group of scenarios was designed to cover for the selection of the target component. Trimetroprim, diclofenac and 17α-ethynylestradiol were tested instead of sulfamethoxazole. Two key aspects are adjusted through the selection of the reference pollutant: the batch time and the reactor volume. The first parameter has a significant influence on the LCA, as it determines the operating time of the lamps and, consequently, the electricity consumption. The reactor volume, in contrast, is not the focus of this study, since its implications are limited to the construction phase, which lies outside the system boundaries. Nevertheless, this may represent a limitation for cost–benefit analyses, as the reactor size could range from 2.4 to 25.7 m^3. The following scenarios were proposed:

1. **PL-TMP:** Modified PL scenario with 80 % removal of trimethoprim. TMP has been chosen since it is the compound with the lowest removal efficiency.
2. **PL-DCF:** Modified PL scenario with 80 % removal of diclofenac. DCF is the compound with the best removal efficiency.
3. **PL-EE2:** Modified PL scenario with 80 % removal of 17α-ethynylestradiol. This scenario aims to analyze the effects of prioritizing the removal of compounds with the most significant environmental damage, based on their LCIA (Life Cycle Impact Assessment) characterization factors.

The second group of scenarios aimed to study the effects of the improvement of light efficiency since the reduction of the light intensity inside the reactor was verified with the PL/2 scenario.

4. **PL/4- Energy:** The energy consumption of the lamps is 25 % of the original PL scenario. The assumption is that the electricity decrease will not affect the kinetics of the process since the light intensity is supposed not to change.
5. **PL/8 - Energy:** Similarly to the previous PL/4 scenario, the energy demand was again reduced to half of the baseline PL scenario.
6. **PL/2-Energy:** The original PL/2 scenario was designed to understand how the photocatalytic reaction was affected by the light intensity inside the reactor. However, the purpose of this scenario is to keep the same light intensity of PL but reduce the energy demand. This could be achieved through the change of the type of lamps of the reactor for others to be more efficient and able to consume less energy from the grid (the half) but resulting in the same light intensity.

Strategies for the target component selection and energy demand variations were also jointly proposed.

7. **PL/2-EE2:** This scenario is similar to scenario PL/2, but with EE2 as the target pollutant to achieve 80 % removal. In this case, light intensity has been modified, affecting the process kinetics.
8. **PL/2-EE2 Energy and PL/4-EE2 Energy:** Similar assumptions have been taken to scenario PL/2-Energy but EE2 is the reference contaminant instead of sulfamethoxazole (the contaminant used in the baseline initially proposed four scenarios). For PL/4-EE2 Energy the electricity demand was reduced to half.

In this regard, the purpose of these three groups of scenarios is to analyze whether the photocatalytic reactor can emerge as a potential technology capable of meeting the removal efficiency thresholds set by Directive (EU) 2024/3019, while ensuring that the indirect impacts do not exceed the damage that could potentially result from inaction.

Finally, and for the catalyst losses, twelve scenarios taking values between 0.05 % and 100 % were proposed to determine relative and absolute variations in the environmental profile of the photocatalytic treatment.

3. Results

3.1. Analysis of inventory

The inventory analysis results for the scale-up scenarios focus on the treatment of hospital wastewater, which was initially processed through a membrane bioreactor (secondary treatment) and subsequently fed into photocatalytic reactors for the removal of residual micropollutants. The LCI is structured into three main categories: energy, chemicals, and emissions.

Among the evaluated scenarios, PL/2 showed the best performance in terms of energy efficiency, with a total consumption of 1.59 kWh/m^3 . In this case, lighting accounted for 53 % of the energy usage. The remaining scenarios exhibited energy consumption approximately 35 % higher, with lighting representing nearly 70 % of the total demand. Specifically, the PL scenario exhibited an energy demand referent to lighting of 1.23 kWh/m^3, a value significantly lower than the values reported for lab-scale photocatalytic systems (44–50,000 kWh/m^3) depending on reactor volume and irradiation configuration. The lower values of that interval have been reported by Tra et al., (2023) and Malakootian et al. (2020), both with systems for a total reaction volume of 2 L and 800 mL respectively.

Therefore, this discrepancy can be attributed to scale effects and design optimization in pilot-scale treatments, which improve light utilization and minimize losses in top- and bottom-irradiated reactors. Although direct comparisons are constrained by the absence of standardized energy reporting in the literature, the findings of this study indicate that the energy consumption obtained is higher than that of conventional UV-based disinfection technologies (around 0.5 kWh/m^3) and in line with photocatalytic systems, approaching the lower boundaries of full-scale (Miklos et al., 2018).

Apart from lighting, other components such as pumps remained consistent across all scenarios, although they still contribute significantly to the overall energy footprint. Scenarios P/2 L and L demonstrated reduced chemical consumption, particularly in terms of hydrogen peroxide, when compared to the baseline PL scenario. These alternatives present more sustainable options from the chemical use perspective.

When it comes to emissions, the results may vary depending on the selected target pollutant. Using sulfamethoxazole as reference (for the baseline scenarios) to achieve the 80 % removal efficiency required by legislation and considering a typical hospital influent (see Table 1), the pollutants of greatest concern in the effluent were trimethoprim and naproxen. The PL scenario showed the highest removal efficiency for these compounds—approximately 21 % for trimethoprim and 46 % for naproxen—followed by P/2 L, with 14 % and 39 % removal, respectively. These results suggest that trimethoprim would have been a more suitable candidate as the reference compound for meeting the 80 % removal threshold. However, prioritizing this compound would significantly extend the operational time—from roughly 40 min to 274 min—requiring a larger reactor volume and substantially increasing energy demand for lighting, reaching up to 14.8 kWh/m^3. Under such conditions, energy consumption would exceed typical values reported in the literature for conventional wastewater treatments that also target nutrient, pathogen, and emerging contaminant (0.5–2.0 kWh/m^3) (Ghimire et al., 2021). On the other hand, it should be taken into account here that a decrease in toxicity from the removal of pollutants, and thus direct emissions, might not be compensated with an indirect contamination by other sources (e.g., electricity and chemicals).

PL is better for the removal of 5 (shown in Table 2) of the 9 micropollutants under assessment while P/2 L is better for 3 of them (estradiol, diclofenac and sulfamethoxazole). It should be considered also that P/2 L is also the second-best scenario for the removal of the 5 contaminants previously mentioned for PL. Indeed, the maximum difference between both scenarios can be found for ibuprofen (23 %), and ciprofloxacin (13 %). The worst removal efficiencies are achieved for the L scenario.

Based on the previously discussed aspects related to energy consumption, chemical use, and emissions, there is no single scenario that clearly outperforms the others across all categories, which creates a certain level of controversy when identifying the most environmentally favorable option. Scenario L performs best in terms of reduced chemical consumption. Scenario PL stands out for its higher removal efficiency and lower emissions, while scenario PL/2 shows the lowest overall energy demand. In this regard, the subsequent Section 3.2 would provide a hotspot analysis and scenario benchmarking considering all the elements together based on the different categories of the EF3.1 method.

3.2. Hotspot and scenario benchmarking

Except for WU and FET, the profile of the photocatalytic process is characterized by the consumption of energy in more than 95 % (shown in Fig. 2). In accordance with the LCI, the lightning has a contribution of around 65 %. The use of pumps represents around 34 %. The chemicals (nanoparticles and hydrogen peroxide) represent less than 2 % in all categories except for WU (85 %) and MRU (5 %). In both scenarios, the main contributor to the environmental impact is the use of nanoparticles, primarily due to an estimated 1 % loss per operational batch that should be replaced. Additional explanations regarding the environmental footprint associated with the nanoparticles are detailed in Feijoo et al. (2017).

In the FET category, the direct effluent emissions may represent around 27 %. However, not all of them have an influence in the same extent. The hormones EE2 and E2 are the concerning pollutants, representing 80 % and 15 % of the effluent emissions. This is contradictory to the information of Table 1, where the hormones represented less than 0.5 % of the mass weight of the emissions. This

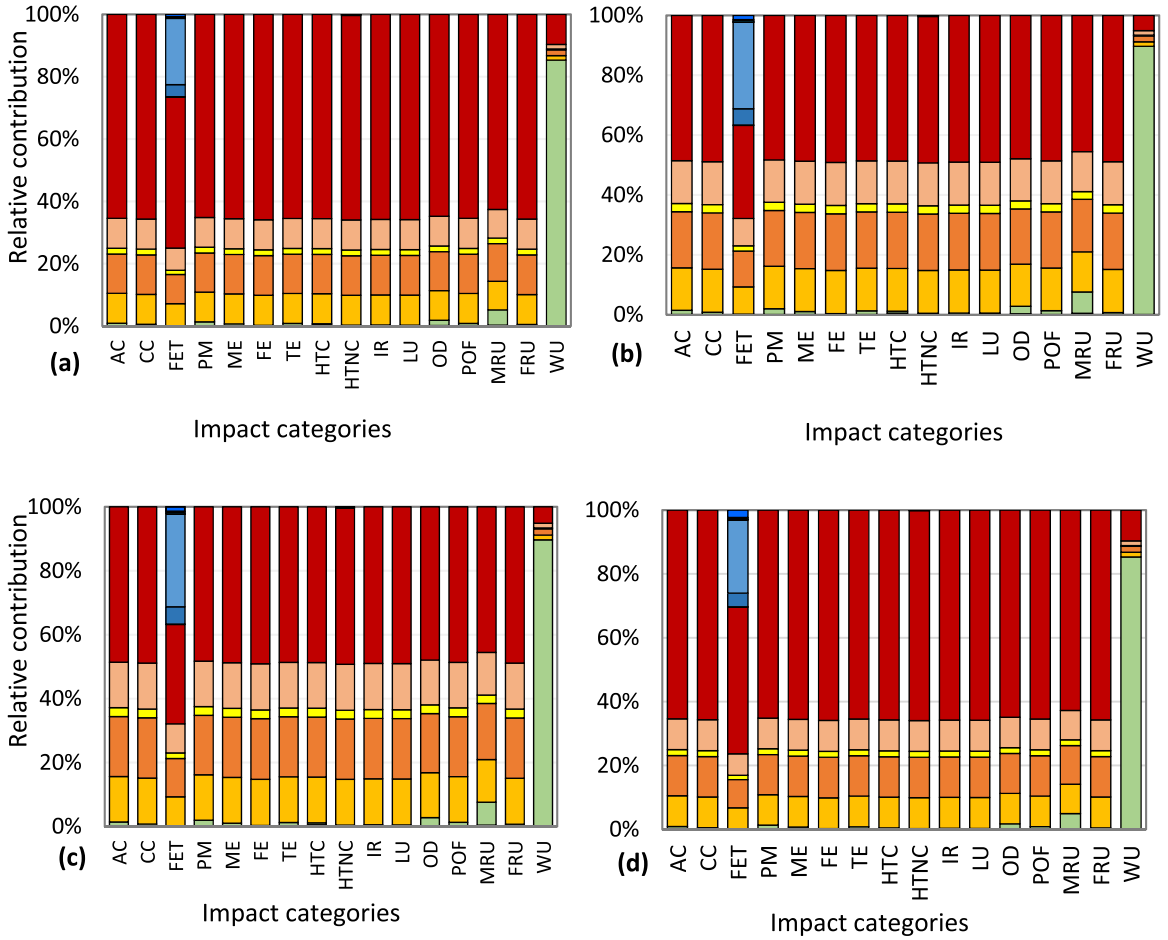

Fig. 2. Relative contribution impact (MidPoint) profile for the PL (a), PL/2 (b), P/2 L (c) and L (d) scenarios. AC: Acidification; CC: Climate Change; FE: Freshwater Eutrophication; FET: Freshwater Ecotoxicity; FRU: Fossil Resource Use; HTC: Human Toxicity Cancer; HTNC: Human Toxicity Non-Cancer; IR: Ionizing Radiation; LU: Land Use; ME: Marine Eutrophication; MRU: Mineral Resource Use; OD: Ozone depletion; PL: 200 mg/L of H_2O_2, 1.12 W/m^2; PL/2: 200 mg/L of H_2O_2, 0.56 W/m^2; P/2 L: 100 mg/L of H_2O_2, 1.12 W/m^2; L: 0 mg/L of H_2O_2, 1.12 W/m^2; PM: Particular Matter; POF: Photochemical Ozone Formation; TE: Terrestrial Eutrophication; WU: Water Use. Hydrogen peroxide; Nanoparticles; Mixing tank; Reactor mixing; Reactor discharge; Buffer tank; Lightning; Estrone; Estradiol; 17α-ethynylestradiol; Ibuprofen; Diclofenac; Naproxen; Sulfamethoxazole; Trimethoprim; Ciprofloxacine; iron oxide emission.

result can be explained by the findings from the LCIA phase. For instance, the characterization factor of E2 is approximately 124 times higher than that of trimethoprim, which is the most concentrated pharmaceutical compound present in the effluent. This is consistent with the relatively low removal efficiencies observed for hormonal compounds, which range from 30 % to 38 % at an operational time of 40 min.

The total FET of the PL scenario is 1.86 CTUe/m^3 for a removal of 80 % of sulfamethoxazole and 0.49 CTUe/m^3 comes from the direct emissions to the environment. The impact of discharging the influent of the photocatalytic reactor to the environment would be 3.64 CTUe/m^3, which is almost 2 times higher than the indirect impacts from the treatment and the effluent release considering only the parent components. This outcome improves significantly in the PL/2 scenario, where lighting energy consumption is reduced by half, achieving a performance that is 2.5 times better.

Although the PL and P/2 L scenarios reach the highest removal efficiencies, as shown in Table 1 and discussed in Section 3.1, the PL/2 scenario demonstrates the most balanced overall behavior. This is due to a compensation between direct emissions and indirect toxicity impacts, which offset each other and lead to a more favorable environmental profile.

Fig. 3 shows how the PL/2, where there is a reduction of the light intensity, has the best outcomes in all of the EF3.1 categories. With the exception of scenario WU, the improvement is approximately 30 %. Another noteworthy finding is that the freshwater ecotoxicity result for scenario P/2 L is 5.2 % lower than that of scenario L. Scenarios PL and P/2 L exhibit similar environmental profiles, with differences smaller than 0.3 %. This suggests that reducing the hydrogen peroxide concentration by half does not lead to significant changes in the environmental impact. However, completely eliminating this oxidizing agent negatively affects the removal efficiency, which in turn increases the freshwater ecotoxicity.

3.3. Results of the sensitivity analysis

As has been already discussed in Section 3.2, all the impact categories are reporting similar results to climate change, with the exception of WU and FET. Therefore, this section will only focus on a deeper investigation of the evolution of the CC and FET categories based on the target pollutant to be removed, the energy consumption in the lamps and the catalyst losses. The goal here is to determine whether the photocatalytic treatment direct and indirect impacts are lower than those potentially generated by an inaction or discharge of the wastewater without treatment.

PL-TMP, PL-DCF and PL-EE2 scenarios of Table 5 are related to the change of the reference pollutant, which is the one that needs to reach 80 % of removal among the mixture of 9 contaminants. The best performance in terms of environmental impact for both CC and FET is PL-DCF. However, this scenario is the worst performing in terms of accomplishment of the legislation thresholds. The reasoning behind this is the inability of the process to achieve the 80 % removal for 7 (except DCF and CPF) of the 9 compounds of the influent wastewater mixture. Although it is the less environmentally friendly scenario, PL-TMP is able to remove all the micropollutants with the minimum desired removal. However, the ecotoxicity implications for the freshwater resources of the installation of such process are 3 times bigger than that of discharging the wastewater directly to the media. Under the current operating conditions of PL, trying to

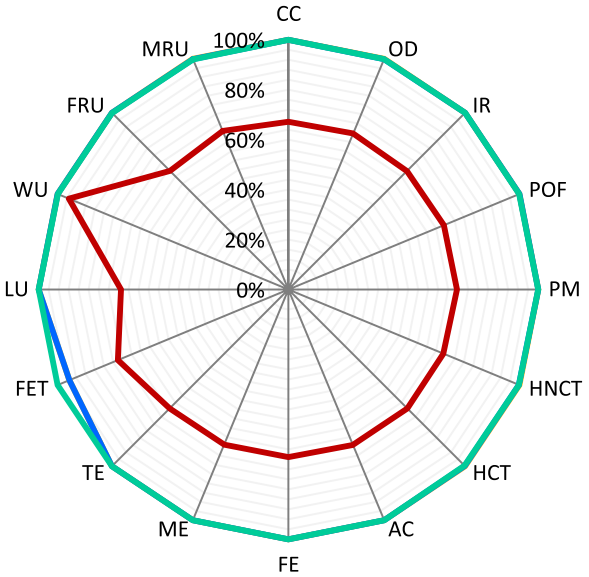

Fig. 3. Relative comparative impact (MidPoint) profile for the PL (), PL/2 (), P/2 L () and L () scenarios. AC: Acidification; CC: Climate Change; FE: Freshwater Eutrophication; FET: Freshwater Ecotoxicity; FRU: Fossil Resource Use; HTC: Human Toxicity Cancer; HTNC: Human Toxicity Non-Cancer; IR: Ionizing Radiation; LU: Land Use; ME: Marine Eutrophication; MRU: Mineral Resource Use; OD: Ozone depletion; PL: 200 mg/L of H_2O_2, 1.12 W/m^2; PL/2: 200 mg/L of H_2O_2, 0.56 W/m^2; P/2 L: 100 mg/L of H_2O_2, 1.12 W/m^2; L: 0 mg/L of H_2O_2, 1.12 W/m^2; PM: Particular Matter; POF: Photochemical Ozone Formation; TE: Terrestrial Eutrophication; WU: Water Use.

Table 5
Climate change and freshwater ecotoxicity absolute MidPoint outcomes for the scenarios proposed for a sensitivity analysis.

Scenarios	CC (kg CO_2eq./m^3)	FET (CTUe/m^3)
Baseline scenarios		
PL	0.62	1.86
PL/2	0.42	1.41
P/2 L	0.62	1.90
L	0.62	1.96
Scenarios with change of target component		
PL - TMP	4.94	10.94
PL - DCF	0.37	1.41
PL - EE2	3.02	6.80
Scenarios with change of electricity		
PL/2 - Energy	0.42	1.41
PL/4 - Energy	0.32	1.18
PL/8 - Energy	0.26	1.07
Strategic combined scenarios		
PL/2 - EE2 Energy	1.81	4.13
PL/2 - EE2	1.81	4.13
PL/4 - EE2 Energy	1.20	2.79

Notes: L: 0 mg/L of H_2O_2, 1.12 W/m^2; PL: 200 mg/L of H_2O_2, 1.12 W/m^2; PL/2: 200 mg/L of H_2O_2, 0.56 W/m^2; P/2 L: 100 mg/L of H_2O_2, 1.12 W/m^2; PL-TMP: PL with trimethoprim as reference; PL-DCF: PL with diclofenac as reference; PL-EE2: PL with 17α-ethynylestradiol as reference; PL/2-Energy: PL with half of energy demand in the lamps; PL/4-Energy: PL with 1/4 of energy demand in the lamps; PL/8-Energy: PL with 1/8 of the energy demand in the lamps; PL/2-EE2: PL with half of energy demand in the lamps and 17α-ethynylestradiol as reference; PL/2 -EE2: PL/2 with 17α-ethynylestradiol as reference; PL/4- EE2 Energy: PL with 1/4 of the energy demand in the lamps and 17α-ethynylestradiol as reference.

achieve 80 % removal of EE2 is still not a good strategy from an environmental perspective with 1.9 more environmental impact than direct discharge. However, the PL-EE2 process allows to satisfactorily remove all contaminants except estradiol and trimethoprim, which has 79 % and 63 % removal efficiencies (relatively close to the legislation-imposed criteria).

Table 5 also shows the results for the scenarios with energy changes in the lamps. For the reference pollutant (SMX), the CC category may vary between 0.26 and 0.62 kg CO_2eq./m^3. The change of the reference pollutant to EE2 report values around 34 % bigger for CC and the PL/2 scenario considering half of the light intensity. In terms of FET, the impact remains approximately 1.14 times higher than taking no action to mitigate the environmental toxicological damage to aquatic ecosystems. To ensure a reasonable operation of the photocatalytic reactor, the recommended solution would be to reduce the electricity consumption of the lamps to one quarter of that used in the current PL scenario, while maintaining the requirement that 80 % of EE2 is removed. Under these conditions, seven out of nine micropollutants would meet the legislative thresholds, with an environmental cost that remains sustainable when compared to the impact of directly discharging the untreated effluent into the environment. The PL/4-EE2 Energy needs, however, the release of 1.2 kg CO_2eq./m^3 while is higher compared to the average expected for conventional domestic WWTPs (~0.30 kg CO_2eq./m^3) (Sala-Garrido et al., 2023). To meet legislative thresholds for all micropollutants while ensuring high environmental protection, additional treatment measures may be proposed, and future research could explore the integration of complementary technologies. In this context, attention should be given not only to treatment systems but also to effective strategies for remediation and risk reduction (Bi et al., 2025; Qu et al., 2024).

Two key aspects influence the catalyst loss rate: (1) indirect impacts from manufacturing and (2) direct effluent emissions caused by inefficiencies in the magnetic recovery system. The CC category is affected only by material consumption, while toxicity-related categories are more sensitive to direct emissions.

For every 1 % loss of catalyst, CC emissions rise by approximately $3.2 \cdot 10^{-3}$ kg CO_2eq./m^3, which can result in an increase of nearly 24 % at maximum loss. This corresponds to up to 33 % of the relative contribution from the photocatalytic process. Under the PL scenario, CC could therefore increase from 0.62 to 0.93 kg CO_2eq./m^3. The trend of CC emissions, along with the relative contribution of Fe_3O_4/ZnO nanoparticles to the overall treatment process is shown in Figs. A2a and A2b (Supplementary Materials A).

When iron oxide is used as the reference material for direct water emissions, human non-cancer ecotoxicity is affected, with a 0.04 % contribution per 1 % catalyst loss. In the extreme case of no catalyst recovery, these emissions could reach up to 3.3 %. However, the EF3.1 method also provides characterization factors for iron (III) emissions instead of iron oxide. Using iron (III) as the reference factor shifts the impact to the freshwater ecotoxicity (FET) category. Here, emissions represent only 0.3 % per 1 % catalyst loss, but the impact becomes more significant at higher losses (e.g., nearly 22 % representativeness at 100 % loss). Further details are presented in **Fig. A2c**.

4. Discussion of results

4.1. The removal efficiency of pharmaceuticals

The main objective of the photocatalytic reactor is to reach an 80 % removal efficiency of micropollutants, as required by Directive (EU) 2024/3019. Nevertheless, the degradation rates associated with photocatalytic technologies do not consistently meet the legislative thresholds for all target compounds. To better understand this limitation, a comprehensive review of 151 studies was carried out. This analysis provided detailed information on the average, maximum, and minimum removal efficiencies achieved using various heterogeneous photocatalysts, offering a valuable benchmark for evaluating the performance of the pilot-scale reactor. Information on removal efficiency, both annually and on average, is provided in Table 6 and, by publication, inTable B1 (in Supplementary Materials B).

As shown in these tables, the average removal efficiency of pharmaceuticals using photocatalysis in literature ranges from 68.3 % (for TMP) to 90.7 % (for E2). Hormones generally exhibit the best performance, with removal efficiencies ranging from 53.3 % to 100 %, while antibiotics can show removal efficiencies as low as 12 %.

It is important to note that the studies compiled in Supplementary Materials B and summarized in Table 6 were not conducted under uniform experimental conditions, as there are no standardized methodologies for assessing micropollutant removal through these types of processes. Furthermore, the reviewed works consider diverse photocatalytic materials, catalyst concentrations, reaction matrix pH levels, and irradiation sources (e.g., UVC, UVB, UVA, artificial visible light, and solar light).

For this reason, the present study adopts a holistic perspective on photocatalytic processes, selecting removal efficiencies obtained under the most favorable experimental conditions and comparing the optimized performance parameters of each proposed technology. The detailed information gathered during the literature review, including initial micropollutant concentrations, material type, catalyst loading, degradation time, pH (when specified), and reaction time, is provided in Table B1 of the Supplementary Materials. Although no standardized testing conditions were identified, typical variable ranges and recurring experimental configurations were observed.

In terms of catalysts, Ti-based materials were the most extensively studied, followed by Bi-based, Fe-based, and carbon nitride materials. The main strategies applied to enhance photocatalytic performance include doping with transition metals (e.g., Fe, Ni, Cu) or non-metals (e.g., N), as well as the development of nanocomposites. The average reaction time reported is approximately 150 min, ranging from 15 min to 10 h. Initial pollutant concentrations typically fall within 10–50 mg/L, while catalyst loadings vary between 0.1 and 6.0 g/L, most frequently around 1 g/L. The irradiation source depends on the material investigated; however, nearly two-thirds of the reviewed studies employ artificial visible light, most commonly using a Xenon lamp equipped with a 400–420 nm cut-off filter. In contrast, the use of natural solar irradiation or direct sunlight accounts for less than 10 % of cases.

A particularly noteworthy finding from the literature is the absence of pilot-scale reactors, with most experiments performed in volumes ranging from 10 mL to 2 L, except for membrane-coupled systems, where treated effluent volumes can reach up to 4 L. In this context, the present study provides a significant contribution by reporting micropollutant removal efficiencies for pilot-scale reactors, thereby bridging the gap between laboratory experimentation and real-world applications of photocatalytic technologies.

The removal efficiencies observed in the baseline scenario PL ranged from 33 % for trimethoprim to 98 % for diclofenac during a 60-minute batch operation of the pilot-scale photocatalytic reactor. In this treatment, the highest efficiencies were obtained for anti-inflammatory drugs, with values between 56 % and 98 %, followed by antibiotics, ranging from 33 % to 94 %. In contrast, hormones showed the lowest removal efficiencies: 43 %-55 %. When scaling up the process for hospital wastewater treatment, overall degradation efficiencies decreased to a range of 21–93 %. This reduction was primarily due to the adjustment of operation time based on the

Table 6
Summary of average, upper and lower removal efficiencies of the selected micropollutants with heterogenous photocatalysis per year.

Year	E1	E2	EE2	IBP	NPX	DCF	SMX	TMP	CPF	Publication (No.)
2024	-	-	-	50.0%	81.8%	74.8%	87.7%	-	79.0%	14
2023	-	86.0%	-	-	-	65.3%	81.2%	-	79.1%	8
2022	-	-	-	-	-	87.6%	62.9%	-	90.2%	14
2021	87.5%	-	-	93.9%	-	-	86.8%	-	94.7%	19
2020	71.1%	-	66.0%	91.2%	-	83.9%	74.0%	87.0%	84.4%	25
2019	-	-	-	89.0%	82.7%	78.8%	73.4%	76.0%	72.1%	25
2018	88.0%	-	-	93.2%	-	62.5%	86.3%	42.5%	-	10
2017	-	-	-	71.4%	-	-	82.5%	84.0%	54.4%	16
Before 2017	95.0%	100.0%	100.0%	80.4%	-	69.0%	53.4%	60.2%	85.4%	20
Median average	82.5%	90.7%	83.0%	85.4%	82.2%	75.8%	76.9%	68.3%	80.7%	-
Upper value	95.0%	100.0%	100.0%	99.9%	82.7%	98.0%	98.8%	87.0%	100.0%	-
Lower value	53.4%	82.0%	66.0%	26.6%	81.8%	47.9%	20.2%	42.5%	12.0%	-

Note: E1: Estrone; E2: Estradiol; EE2: 17α-ethynylestradiol; IBP: Ibuprofen; NPX: Naproxen; DCF: Diclofenac; SMX: Sulfamethoxazole; TMP: Trimethoprim; CPF: Ciprofloxacin.

selection of a target pollutant required to meet a minimum removal threshold of 80 %.

According to first-order degradation kinetics, all micropollutants could reach at least 80 % removal with approximately 4.5 h of operation. This observation underscores the importance of correlating removal efficiency with the corresponding residence time and associated resource consumption. Although the efficiencies reported in this study are consistent with those in the literature, direct comparisons cannot be made without considering the required operation time to achieve them.

4.2. The performance of photocatalysis with a literature overview

According to the literature, the environmental performance of photocatalysis is proportionally energy-dependent, while the impact of reagents and catalysts is relatively low in comparison. Thus, the lower the energy consumption, the better the environmental profile (Chatzisymeon et al., 2013). Reported results indicate that electricity may contribute up to 93 % of the climate change compared to other inventory components (Muñoz et al., 2005). The most contributing factors are the lamps that ensure light irradiation, and the stirrers used for catalyst mixing (Foteinis et al., 2018). The research presented in this manuscript aligns with these outcomes of the literature since the energy consumption of the lamps is the main contributor and also the energy represents more than 95 %. Therefore, the use of more energy-efficiency lamps should be promoted. Another strategy, as analyzed by Muñoz et al. (2006), could the use of solar renewable electricity in the lamps. Based on the outcomes achieved by these authors, this action may reduce the environmental impact by more than 90 % during operation. Considering that this result could also be obtained if solar energy were used a feasible scenario for the photocatalytic system study in this research, the minimum climate change impact that could be hypothetically reached is 0.12 kg CO_2eq./m^3. ("PL/4-EE2 Energy" with solar energy).

Among processes with similar electricity demands, the differences in the operation of photocatalytic alternatives of the literature are influenced by the use of chemicals and the efficiency of the catalyst. The impact of the chemicals has been verified through the comparison of the scenario PL, P/2 L and L, reporting similar conclusions as those from previously indicated in the literature.

Although catalysts have a greater indirect environmental impact from their manufacturing than other reagents, they reduce treatment time and thus decrease the operation times of the most energy-consuming components. However, the environmental benefits of the catalyst are not realized if it is not recovered and reused for more than one treatment cycle. If this does not occur, the consumption of the catalyst becomes the primary environmental influence. In this regard, Magdy et al. (2021) found that for TiO_2, the contribution of the catalyst could be more than 80 %. Therefore, minimizing the environmental impacts of the catalyst depends on selecting the optimal concentration, ensuring its reusability for multiple cycles, improving its production process, and enhancing its efficiency (the latter two aspects are also related to the materials used in its composition) (Costamagna et al., 2020). In this regard, the optimization of the concentration of the magnetic catalysts and reuse among cycles (with the exception of losses) for this study has resulted in a remarkable impact only for the category of water use while its effect was completely negligible for the remaining categories.

4.3. The photocatalytic treatment compared with other alternatives

The studies analyzing the environmental profile of photocatalysis using LCA have two distinct goals. On one hand, they aim to explore the effects of using hydrogen peroxide as a reagent and the impact of two light sources (electrical and solar). On the other hand, these technologies are compared to three other advanced oxidation processes: photo-Fenton, electro-Fenton, and adsorption. However, only in one study a combination of the photocatalysis with one of the previous mentioned (photo-Fenton) technologies was addressed (Muñoz et al., 2005). For both approaches, Table 7 compiles the results of those publications, providing results for the categories with common units among this research another (climate change, freshwater eutrophication and ozone depletion), expressed per cubic meter of wastewater treated. Since the units for many categories do not align, the outcomes for the remaining categories were provided in Table A2. In photocatalysis the CC ranges between $2.49{\cdot}10^{-2}$ and 90 kg CO_2eq./m^3. The bigger values were found for Muñoz et al. (2005) since the goal of the photocatalytic technology was the treatment of a highly concentrated stream, kraft pulp mill wastewater.

Table 7
Environmental impacts of photocatalytic processes from Life Cycle Assessment literature and wastewater treatment for those impact categories with common units (per m^3 of wastewater treated).

Technology/Impact category		Climate change (kg CO_2eq.)	Freshwater eutrophication (kg P eq.)	Ozone depletion (μg CFC_{-11} eq.)
Photocatalysis	With electricity	[1]5.26 [2]90 [3]0.11 [4]4.08	[1]0.63 [2]14 [3]$4.69{\cdot}10^{-2}$ [4]$1.89{\cdot}10^{-3}$	[1]35.05 [2]22,000 [4]586
	With solar energy	[1]5.13 [2]0.48	[1]0.61 [2]$7.8{\cdot}10^{-2}$	[1]34.28 [2]76
	With ultraviolet energy	[1]5.17	[1]0.62	[1]34.3
	With electricity and H_2O_2	[2]54 [3]0.135	[2]8.5 [3]$5.72{\cdot}10^{-2}$	[2]13,000
	With solar energy and H_2O_2	[2]1.2 [3]$2.49{\cdot}10^{-2}$	[2]0.37 [3]$1.02{\cdot}10^{-2}$	[2]89
Photo-Fenton	With electricity	[2]38 [4]0.88	[2]6 [4]0.15	[2]9000 [4]87.5
	With solar energy	[2]0.76	[2]0.3	[2]38
Photo-Fenton followed by photocatalysis		[2]1.2–16	[2]2.7–3.7	[2]90–3700
Electro-Fenton		[4]26.78	[4]7.33	[4]1610
Adsorption		[4]5.12	[4]35.27	[4]6750

Note: The numerical superscripts indicate the bibliographic reference from where the data was taking from: (1) Pesqueira et al. (2024), (2) Muñoz et al. (2005), (3) Pesqueira et al. (2021), (4) Magdy et al. (2021).

This interval of smaller for photocatalysis with electricity and use of hydrogen peroxide (0.135–54 kg CO_2eq./m^3). The results reported within this investigation were around 0.26–4.94 kg CO_2eq./m^3, which means that the technology is in line with literature and could be competitive with the current solar energy photocatalysis, photo Fenton, electro-Fenton and adsorption. Below there is an explanation of the goals previously mentioned of the bibliographic studies found:

4.3.1. Effects of the use of hydrogen peroxide

There is no current consensus on the use of this reagent in photocatalytic processes. Muñoz et al. (2005) showed that for a concentrated stream, such as kraft mill bleaching wastewater, photocatalytic processes that do not consume chemicals are reported to be more environmentally friendly due to the absence of indirect impacts from chemical manufacturing. On the other hand, effluents from secondary treatment improved their environmental profile with the use of H_2O_2 (Pesqueira et al., 2021). Although this research also has a treatment for a diluted stream, the outcomes achieved indicate that the use of hydrogen peroxide is not relevant in terms of environmental profile. This is indicative that three tendencies can be identified when it comes to the friendliness of the use of hydrogen peroxide.

4.3.2. Selection of light sources

Regardless of the irradiation source, the use of non-renewable energy results in a greater environmental impact (Dubsok et al., 2022). The type of irradiation also influences the environmental performance of the system. UV-A irradiation has been reported to have a significantly larger environmental impact than UV-C irradiation. This difference is expected, as UV-C treatment operates at a much faster treatment rate (Foteinis et al., 2018). The presented photocatalytic process is operating with UV-A irradiation which implies that there is still room for improvement on the environmental profile of the technology.

4.3.3. Comparison with other technologies

For the treatment of α-methyl-phenylglycine the use of solar photo-Fenton was better than that of coupling heterogeneous photocatalysis because of the lower use of electricity (Muñoz et al., 2006). In the treatment of kraft mill bleaching wastewaters, heterogeneous photocatalysis was the best option followed by photo-Fenton, photocatalysis with the use of hydrogen peroxide and a combination of the two technologies (Muñoz et al., 2005). For Olive mill wastewater, the best option was electrochemical oxidation followed by wet air oxidation and heterogeneous photocatalysis linked again by the use of electricity (Chatzisymeon et al., 2013). If the pollutant is phenolic wastewater, electro-Fenton was the least environmentally friendly technology, and the best one was solar photo-Fenton. From better to worse, other technologies analyzed for this pollutant were also solar photocatalysis, adsorption and a combination of photocatalysis with activated carbon. Compared to the previously presented concentrated streams, removal of micropollutants (carbamazepine, diclofenac and sulfamethoxazole; 5 μg/L) from a secondary-treated wastewater resulted in the subsequent raking of technologies: circumneutral photo-Fenton, photocatalysis with TiO_2 and hydrogen peroxide, photocatalysis with TiO_2, solar photolysis with hydrogen peroxide and solar photocatalysis (Pesqueira et al., 2021). Considering the current state-of-the art photo-Fenton seems to be in a good position towards lowering environmental emissions while the application of photocatalysis is still controversial. Therefore, improvements in the process should be made to reduce the current value shown in Table 7. On the other hand, some aspects are missing from environmental research of photocatalytic technologies: the influence of the wastewater concentration on the profile and recalcitrant characteristics of the compounds.

5. Conclusions

A photocatalytic reactor was successfully scaled-up and implemented for the treatment of effluent from a membrane reactor at an average-size Spanish hospital. The environmental profile of the technology was assessed, considering an effluent mixture composed of nine micropollutants, including anti-inflammatories, hormones, and antibiotics. The photocatalytic process was primarily characterized by its energy demand, with more than 95 % of the energy consumption attributed to the electricity used by the lamps. Notably, variations in the energy consumption of the lamps may result variations in the climate change between 0.26 and 1.81 kg CO_2eq./m^3 and 1.4–4.2 CTUe/m^3 for freshwater ecotoxicity. The energy consumption of the lamps emerged as a key factor determining the success of the photocatalytic process in yielding better outcomes than the direct discharge of polluted wastewater, which has an impact of 3.6 CTUe/m^3 . This is particularly crucial considering the legislative requirements, which require a removal efficiency of over 80 % for micropollutants. The challenges in achieving such removal efficiencies could lead to increased indirect impacts, potentially resulting in higher ecotoxicities than the direct discharge scenario. To align with both legislative goals and minimize environmental impact, this study underscores the importance of selecting a reference micropollutant. This choice has a significant influence on operational times and, consequently, the energy demand of the process. Based on this analysis, the optimal scenario should prioritize the removal of the hormone EE2 by 80 % while ensuring the process consumes less than 0.8 kWh/m^3.

CRediT authorship contribution statement

Jorge González-Rodríguez: Writing – original draft, Investigation, Formal analysis. **Isabella Narváez-Prado:** Investigation, Formal analysis. **Estévez Rivadulla Sofía:** Writing – original draft, Visualization, Methodology, Investigation, Formal analysis. **Feijoo Costa Gumersindo:** Writing – review & editing, Validation, Supervision. **Moreira Maria Teresa:** Writing – review & editing, Validation, Supervision.

Declaration of Competing Interest

The authors declare the following financial interests/personal relationships which may be considered as potential competing interests: Sofia Estevez Rivadulla and Isabella Narváez Prado reports financial support was provided by Spanish Ministry of Science, Innovation and Universities and Jorge González-Rodríguez reports financial support was provided by Xunta de Galicia. Sofia Estevez Rivadulla and Isabella Narváez Prado reports financial support was provided CIES (PID2022–142334OB-I00) project, granted by MCIN/ AEI /10.13039/501100011033/. If there are other authors, they declare that they have no known competing financial interests or personal relationships that could have appeared to influence the work reported in this paper.

Acknowledgements

This research was supported by CIES (PID2022–142334OB-I00) project granted by MCIN/ AEI /10.13039/501100011033/. S. Estévez also thanks the Spanish Ministry of Science, Innovation and Universities for financial support (Grant reference PRE2020–092074). I. Narváez-Prado would also like to thank the Ministry of Science, Innovation and Universities for the support provided with the pre-doctoral grant with reference PREP2022–000851. J. González-Rodríguez thanks Xunta de Galicia for financial support (Grant reference ED481B 2025/070). S. Estévez, J. González-Rodríguez, I. Narváez-Prado, G. Feijoo, and M.T. Moreira authors belong to the Galician Competitive Research Group (GRC ED431C 2021/37) and the Cross-disciplinary Research in Environmental Technologies (CRETUS Research Center, ED431G 2023/12).

Appendix A. Supporting information

Supplementary data associated with this article can be found in the online version at doi:10.1016/j.eti.2025.104617.

Data Availability

Data will be made available on request.

References

Ajala, O.J., Tijani, J.O., Salau, R.B., Abdulkareem, A.S., Aremu, O.S., 2022. A review of emerging micro-pollutants in hospital wastewater: environmental fate and remediation options. Results Eng. 16, 100671. https://doi.org/10.1016/j.rineng.2022.100671.

An, S., Nam, S.-N., Choi, J.S., Park, C.M., Jang, M., Lee, J.Y., Jun, B.-M., Yoon, Y., 2024. Ultrasonic treatment of endocrine disrupting compounds, pharmaceuticals, and personal care products in water: an updated review. J. Hazard. Mater. 474, 134852. https://doi.org/10.1016/j.jhazmat.2024.134852.

Anucha, C.B., Altin, I., Bacaksız, E., Kucukomeroglu, T., Belay, M.H., Stathopoulos, V.N., 2021. Enhanced photocatalytic activity of $CuWO_4$ doped TiO_2 photocatalyst towards carbamazepine removal under UV irradiation. Separations 8 (3), 25. https://doi.org/10.3390/separations8030025.

Archer, E., Petrie, B., Kasprzyk-Hordern, B., Wolfaardt, G.M., 2017. The fate of pharmaceuticals and personal care products (PPCPs), endocrine disrupting contaminants (EDCs), metabolites and illicit drugs in a WWTW and environmental waters. Chemosphere 174, 437–446. https://doi.org/10.1016/j.chemosphere.2017.01.101.

aus der Beek, T., Weber, F., Bergmann, A., Hickmann, S., Ebert, I., Hein, A., Küster, A., 2016. Pharmaceuticals in the environment—global occurrences and perspectives. Environ. Toxicol. Chem. 35 (4), 823–835. https://doi.org/10.1002/etc.3339.

Bi, F., Jiang, Z., Wang, M., Lin, Q., Liu, X., Fu, L., Fan, H., Cao, W., Qu, J., Zhang, Y., 2025. Enhanced remediation of cadmium-contaminated farmland by smooth vetch (*Vicia villosa* var.) coupled with phosphorus/sulfur co-doped biochar: synergetic performance and mechanism. J. Clean. Prod. 496, 144986. https://doi.org/10.1016/j.jclepro.2025.144986.

Blum, K.M., Andersson, P.L., Ahrens, L., Wiberg, K., Haglund, P., 2018. Persistence, mobility and bioavailability of emerging organic contaminants discharged from sewage treatment plants. Sci. Total Environ. 612, 1532–1542. https://doi.org/10.1016/j.scitotenv.2017.09.006.

Bulle, C., Margni, M., Patouillard, L., Boulay, A.-M., Bourgault, G., De Bruille, V., Cao, V., Hauschild, M., Henderson, A., Humbert, S., Kashef-Haghighi, S., Kounina, A., Laurent, A., Levasseur, A., Liard, G., Rosenbaum, R.K., Roy, P.-O., Shaked, S., Fantke, P., Jolliet, O., 2019. IMPACT World+: a globally regionalized life cycle impact assessment method. Int. J. Life Cycle Assess. 24 (9), 1653–1674. https://doi.org/10.1007/s11367-019-01583-0.

Carraro, E., Bonetta, Si., Bertino, C., Lorenzi, E., Bonetta, Sa., Gilli, G., 2016. Hospital effluents management: chemical, physical, microbiological risks and legislation in different countries. J. Environ. Manag. 168, 185–199. https://doi.org/10.1016/j.jenvman.2015.11.021.

Chatzisymeon, E., Foteinis, S., Mantzavinos, D., Tsoutsos, T., 2013. Life cycle assessment of advanced oxidation processes for olive mill wastewater treatment. J. Clean. Prod. 54, 229–234. https://doi.org/10.1016/j.jclepro.2013.05.013.

Chen, L., Feng, Y., He, J., Zhang, Q., Han, L., 2023. Unraveling the effect of continuously accumulating microplastics on the humification of dissolved organic matter in the composting system. ACS EST Eng. 3 (6), 811–822. https://doi.org/10.1021/acsestengg.2c00411.

Costamagna, M., Ciacci, L., Paganini, M.C., Calza, P., Passarini, F., 2020. Combining the highest degradation efficiency with the lowest environmental impact in zinc oxide based photocatalytic systems. J. Clean. Prod. 252, 119762. https://doi.org/10.1016/j.jclepro.2019.119762.

Crater, J.S., Lievense, J.C., 2018. Scale-up of industrial microbial processes. FEMS Microbiol. Lett. 365 (13). https://doi.org/10.1093/femsle/fny138.

Dawood, A.H., Aziz, S.Q., Ismael, S.O., 2023. A review on pharmaceutical wastewater characteristics, treatment techniques and reusing. Environ. Prot. Res. 3 (1), 181–193. https://doi.org/10.37256/epr.3120232273.

de Simone Souza, H.H., Falqui, L., Xuereb, R., Mamo, J., Abela, S., Grech, M., Refalo, P., 2023. Environmental assessment of a single-family photocatalytic greywater treatment system based on the design and operating conditions. Sustain. Prod. Consum. 35, 483–494. https://doi.org/10.1016/j.spc.2022.12.001.

Dominguez, S., Laso, J., Margallo, M., Aldaco, R., Rivero, M.J., Irabien, Á., Ortiz, I., 2018. LCA of greywater management within a water circular economy restorative thinking framework. Sci. Total Environ. 621, 1047–1056. https://doi.org/10.1016/j.scitotenv.2017.10.122.

Dubsok, A., Khamdahsag, P., Kittipongvises, S., 2022. Life cycle environmental impact assessment of cyanate removal in mine tailings wastewater by nano-TiO_2/$FeCl_3$ photocatalysis. J. Clean. Prod. 366, 132928. https://doi.org/10.1016/j.jclepro.2022.132928.

El-Fawal, E.M., Younis, S.A., Zaki, T., 2020. Designing $AgFeO_2$-graphene/$Cu_2(BTC)_3$ MOF heterojunction photocatalysts for enhanced treatment of pharmaceutical wastewater under sunlight. J. Photochem. Photobiol. A Chem. 401, 112746. https://doi.org/10.1016/j.jphotochem.2020.112746.

Elhami, M., Bahramifar, N., Bijanzadeh, H.R., Abyar, H., 2023. Process efficiency and life cycle assessment of novel waste-derived Chl/TiO_2 photocatalyst for rhodamine B removal. J. Water Process Eng. 56, 104425. https://doi.org/10.1016/j.jwpe.2023.104425.

Elshypany, R., Selim, H., Zakaria, K., Moustafa, A.H., Sadeek, S.A., Sharaa, S.I., Raynaud, P., Nada, A.A., 2021. Elaboration of Fe_3O_4/ZnO nanocomposite with highly performance photocatalytic activity for degradation methylene blue under visible light irradiation. Environ. Technol. Innov. 23, 101710. https://doi.org/10.1016/j.eti.2021.101710.

European Council, 2024. Wastewater treatment ⟨https://www.consilium.europa.eu/en/policies/wastewater-treatment⟩.

Feijoo, S., González-García, S., Moldes-Diz, Y., Vazquez-Vazquez, C., Feijoo, G., Moreira, M.T., 2017. Comparative life cycle assessment of different synthesis routes of magnetic nanoparticles. J. Clean. Prod. 143, 528–538. https://doi.org/10.1016/j.jclepro.2016.12.079.

Fernández, L., González-Rodríguez, J., Gamallo, M., Vargas-Osorio, Z., Vázquez-Vázquez, C., Piñeiro, Y., Rivas, J., Feijoo, G., Moreira, M.T., 2020. Iron oxide-mediated photo-Fenton catalysis in the inactivation of enteric bacteria present in wastewater effluents at neutral pH. Environ. Pollut. 266, 115181. https://doi.org/10.1016/j.envpol.2020.115181.

Finnveden, G., Potting, J., 2014. Life cycle assessment. Encyclopedia Toxicology Third Edition 74–77. https://doi.org/10.1016/B978-0-12-386454-3.00627-8.

Foteinis, S., Borthwick, A.G.L., Frontistis, Z., Mantzavinos, D., Chatzisymeon, E., 2018. Environmental sustainability of light-driven processes for wastewater treatment applications. J. Clean. Prod. 182, 8–15. https://doi.org/10.1016/j.jclepro.2018.02.038.

Frederichi, D., Scaliante, M.H.N.O., Bergamasco, R., 2021. Structured photocatalytic systems: photocatalytic coatings on low-cost structures for treatment of water contaminated with micropollutants—a short review. Environ. Sci. Pollut. Res. 28 (19), 23610–23633. https://doi.org/10.1007/s11356-020-10022-9.

Gamallo, M., Fernández, L., Vázquez-Vázquez, C., Fondado, A., Mira, J., Feijoo, G., Moreira, M.T., 2018. Development of a novel magnetic reactor based on nanostructured Fe_3O_4@PAA as heterogenous fenton catalyst. Catalysts 9 (1), 18. https://doi.org/10.3390/catal9010018.

Gamallo, M., Fernández, L., Vázquez-Vázquez, C., Fondado, A., Mira, J., Feijoo, G., Moreira, M.T., 2019. Development of a novel magnetic reactor based on nanostructured Fe_3O_4@PAA as heterogeneous Fenton catalyst. Catalysts 9 (1), 18. https://doi.org/10.3390/catal9010018.

Gaw, S., Thomas, K.V., Hutchinson, T.H., 2014. Sources, impacts and trends of pharmaceuticals in the marine and coastal environment. Philos. Trans. R. Soc. B Biol. Sci. 369 (1656), 20130572. https://doi.org/10.1098/rstb.2013.0572.

Ghazal, H., Koumaki, E., Hoslett, J., Malamis, S., Katsou, E., Barcelo, D., Jouhara, H., 2022. Insights into current physical, chemical and hybrid technologies used for the treatment of wastewater contaminated with pharmaceuticals. J. Clean. Prod. 361, 132079. https://doi.org/10.1016/j.jclepro.2022.132079.

Ghimire, U., Sarpong, G., Gude, V.G., 2021. Transitioning wastewater treatment plants toward circular economy and energy sustainability. ACS Omega 6 (18), 11794–11803. https://doi.org/10.1021/acsomega.0c05827.

Giménez, J., Bayarri, B., González, Ó., Malato, S., Peral, J., Esplugas, S., 2015. Advanced oxidation processes at laboratory scale: environmental and economic impacts. ACS Sustain. Chem. Eng. 3 (12), 3188–3196. https://doi.org/10.1021/acssuschemeng.5b00778.

González-Rodríguez, J., Fernández, L., Vargas-Osorio, Z., Vázquez-Vázquez, C., Piñeiro, Y., Rivas, J., Feijoo, G., Moreira, M.T., 2021a. Reusable Fe_3O_4/SBA15 nanocomposite as an efficient photo-fenton catalyst for the removal of sulfamethoxazole and orange II. Nanomaterials 11 (2), 533. https://doi.org/10.3390/nano11020533.

González-Rodríguez, J., Gamallo, M., Conde, J.J., Vargas-Osorio, Z., Vázquez-Vázquez, C., Piñeiro, Y., Rivas, J., Feijoo, G., Moreira, M.T., 2021b. Exploiting the potential of supported magnetic nanomaterials as fenton-like catalysts for environmental applications. Nanomaterials 11 (11), 2902. https://doi.org/10.3390/nano11112902.

Grand View Research, 2025. Pharmaceutical market size, share & trends analysis report by molecule type, by product, by type, by disease, by formulation, by age group, by route of administration, by end market, by region, and segment forecasts, 2023 - 2030. ⟨https://www.grandviewresearch.com/industry-analysis/pharmaceutical-market-report⟩.

Guerra, M.M., Arrieta Pérez, R., Colina Marquez, J., 2019. Modeling of a solar heterogeneous photocatalytic reactor with TiO_2 for treatment of wastewater contaminated by Albendazole. Ing. ía Y. Compet. 21 (2). https://doi.org/10.25100/iyc.v22i2i.8105.

Hernández-Tenorio, R., González-Juárez, E., Guzmán-Mar, J.L., Hinojosa-Reyes, L., Hernández-Ramírez, A., 2022. Review of occurrence of pharmaceuticals worldwide for estimating concentration ranges in aquatic environments at the end of the last decade. J. Hazard. Mater. Adv. 8, 100172. https://doi.org/10.1016/j.hazadv.2022.100172.

Ibhadon, A., Fitzpatrick, P., 2013. Heterogeneous photocatalysis: recent advances and applications. Catalysts 3 (1), 189–218. https://doi.org/10.3390/catal3010189.

Iervolino, G., Zammit, I., Vaiano, V., Rizzo, L., 2020. Limitations and prospects for wastewater treatment by UV and visible-light-active heterogeneous photocatalysis: a critical review. Top. Curr. Chem. 378 (1), 7. https://doi.org/10.1007/s41061-019-0272-1.

IPCC. 2019. 2019 Refinement to the 2006 IPCC Guidelines for National Greenhouse Gas Inventories. Volume 5, chapter 6. ⟨https://www.ipcc-nggip.iges.or.jp/public/2019rf/pdf/5_Volume5/19R_V5_6_Ch06_Wastewater.pdf⟩.

ISO, 2006. ISO 14040:2006. Environmental management — Life cycle assessment — Principles and framework.

Iyyappan, J., Gaddala, B., Gnanasekaran, R., Gopinath, M., Yuvaraj, D., Kumar, V., 2024. Critical review on wastewater treatment using photo catalytic advanced oxidation process: role of photocatalytic materials, reactor design and kinetics. Case Stud. Chem. Environ. Eng. 9, 100599. https://doi.org/10.1016/J.CSCEE.2023.100599.

Kayode-Afolayan, S.D., Ahuekwe, E.F., Nwinyi, O.C., 2022. Impacts of pharmaceutical effluents on aquatic ecosystems. Sci. Afr. 17, e01288. https://doi.org/10.1016/j.sciaf.2022.e01288.

Khan, M.T., Shah, I.S., Ihsanullah, I., Naushad, M., Ali, S., Shah, S.H.A., Mohammad, A.W., 2021. Hospital wastewater as a source of environmental contamination: an overview of management practices, environmental risks, and treatment processes. J. Water Process Eng. 41, 101990. https://doi.org/10.1016/j.jwpe.2021.101990.

Kong, K., Weng, Y., Lam, W.H., Lai, S.Y., 2023. Environmental footprint assessment of methylene blue photodegradation using graphene-based titanium dioxide. Bull. Chem. React. Eng. Catal. 18 (1), 103–117. https://doi.org/10.9767/bcrec.17450.

Krishnan, R.Y., Manikandan, S., Subbaiya, R., Biruntha, M., Govarthanan, M., Karmegam, N., 2021. Removal of emerging micropollutants originating from pharmaceuticals and personal care products (PPCPs) in water and wastewater by advanced oxidation processes: a review. Environ. Technol. Innov. 23, 101757. https://doi.org/10.1016/j.eti.2021.101757.

Ma, C., Yu, Z., Wei, J., Tan, C., Yang, X., Wang, T., Yu, G., Zhang, C., Li, X., 2022. Metal-free ultrathin C3N5 photocatalyst coupling sodium percarbonate for efficient sulfamethoxazole degradation. Appl. Catal. B Environ. 319, 121951. https://doi.org/10.1016/j.apcatb.2022.121951.

Magdy, M., Gar Alalm, M., El-Etriby, H.K., 2021. Comparative life cycle assessment of five chemical methods for removal of phenol and its transformation products. J. Clean. Prod. 291, 125923. https://doi.org/10.1016/j.jclepro.2021.125923.

Majumder, A., Gupta, A.K., Ghosal, P.S., Varma, M., 2021. A review on hospital wastewater treatment: a special emphasis on occurrence and removal of pharmaceutically active compounds, resistant microorganisms, and SARS-CoV-2. J. Environ. Chem. Eng. 9 (2), 104812. https://doi.org/10.1016/J.JECE.2020.104812.

Malakootian, M., Nasiri, A., Amiri Gharaghani, M., 2020. Photocatalytic degradation of ciprofloxacin antibiotic by TiO_2 nanoparticles immobilized on a glass plate. Chem. Eng. Commun. 207 (1), 56–72. https://doi.org/10.1080/00986445.2019.1573168.

Manickum, T., John, W., 2014. Occurrence, fate and environmental risk assessment of endocrine disruption compounds at the wastewater treatment works is Pietermaritzburg (South Africa). Sci. Total Environ. 468-469, 584–597. https://doi.org/10.1016/j.scitotenv.2013.08.041.

Massart, R., 1981. Preparation of aqueous magnetic liquids in alkaline and acidic media. IEEE Trans. Magn. 17 (2), 1247–1248. https://doi.org/10.1109/TMAG.1981.1061188.

Menéndez-Pedriza, A., Jaumot, J., 2020. Interaction of environmental pollutants with microplastics: a critical review of sorption factors, bioaccumulation and ecotoxicological effects. Toxics 8 (2), 40. https://doi.org/10.3390/toxics8020040.

Merchant, A.I., Vakili, A.H., Kocaman, A., Abu Amr, S.S., 2024. New advancement of advanced oxidation processes for the treatment of Petroleum wastewater. Desalin. Water Treat. 319, 100565. https://doi.org/10.1016/j.dwt.2024.100565.

Miettinen, M., Khan, S.A., 2022. Pharmaceutical pollution: a weakly regulated global environmental risk. Rev. Eur. Comp. Int. Environ. Law 31 (1), 75–88. https://doi.org/10.1111/reel.12422.
Miklos, D.B., Remy, C., Jekel, M., Linden, K.G., Drewes, J.E., Hübner, U., 2018. Evaluation of advanced oxidation processes for water and wastewater treatment – a critical review. Water Res. 139, 118–131. https://doi.org/10.1016/j.watres.2018.03.042.
Ministerio de Sanidad. 2023. Informe anual del sistema nacional de salud 2022. ⟨https://www.sanidad.gob.es/estadEstudios/estadisticas/sisInfSanSNS/tablasEstadisticas/InfAnualSNS2022/INFORME_ANUAL_2022.pdf⟩.
Mitra, S., Chakraborty, A.J., Tareq, A.M., Emran, T.B., Nainu, F., Khusro, A., Idris, A.M., Khandaker, M.U., Osman, H., Alhumaydhi, F.A., Simal-Gandara, J., 2022. Impact of heavy metals on the environment and human health: novel therapeutic insights to counter the toxicity. J. King Saud. Univ. Sci. 34 (3), 101865. https://doi.org/10.1016/j.jksus.2022.101865.
Muñoz, I., Peral, J., Antonio Ayllón, J., Malato, S., Passarinho, P., Domènech, X., 2006. Life cycle assessment of a coupled solar photocatalytic–biological process for wastewater treatment. Water Res. 40 (19), 3533–3540. https://doi.org/10.1016/j.watres.2006.08.001.
Muñoz, I., Rieradevall, J., Torrades, F., Peral, J., Domènech, X., 2005. Environmental assessment of different solar driven advanced oxidation processes. Sol. Energy 79 (4), 369–375. https://doi.org/10.1016/j.solener.2005.02.014.
Mwizerwa, I.T., Sun, Z., Huang, T., Tang, J., Hasan, I.M., Zhao, X., 2024. Single atom photocatalytic micropollutants degradation performance: a review. Desalin. Water Treat. 320, 100656. https://doi.org/10.1016/j.dwt.2024.100656.
Paulu, A., Bartáček, J., Šerešová, M., Kočí, V., 2021. Combining process modelling and LCA to assess the environmental impacts of wastewater treatment innovations. Water 13 (9), 1246. https://doi.org/10.3390/w13091246.
Pavlović, J., Tušar, N.N., Rajić, N., 2024. The synthesis and photocatalytic efficacy of distinct nano-oxides in the breakdown of organic contaminants. Catalysts 14 (11), 771. https://doi.org/10.3390/catal14110771.
Pesqueira, J.F.J.R., Pereira, M.F.R., Silva, A.M.T., 2021. A life cycle assessment of solar-based treatments (H_2O_2, TiO_2 photocatalysis, circumneutral photo-Fenton) for the removal of organic micropollutants. Sci. Total Environ. 761, 143258. https://doi.org/10.1016/j.scitotenv.2020.143258.
Pesqueira, J.F.J.R., Pereira, M.F.R., Silva, A.M.T., 2024. Carbon-based composites in advanced wastewater treatment: a life cycle assessment of TiO_2 and GO-TiO_2 solar photocatalysis. J. Clean. Prod. 444, 140845. https://doi.org/10.1016/j.jclepro.2024.140845.
Pré Sustainability, 2024. SimaPro 9. 6. ⟨https://simapro.com/wp-content/uploads/2024/04/SimaPro960WhatIsNew.pdf⟩.
Qu, J., Li, Y., Bi, F., Liu, X., Dong, Z., Fan, H., Yin, M., Fu, L., Cao, W., Zhang, Y., 2024. Smooth vetch (*Vicia villosa* var.) coupled with ball-milled composite mineral derived from shell powder and phosphate rock for remediation of cadmium-polluted farmland: insights into synergetic mechanisms. ACS EST Eng. 4 (8), 2054–2067. https://doi.org/10.1021/acsestengg.4c00177.
Ruziwa, D.T., Oluwalana, A.E., Mupa, M., Meili, L., Selvasembian, R., Nindi, M.M., Sillanpaa, M., Gwenzi, W., Chaukura, N., 2023. Pharmaceuticals in wastewater and their photocatalytic degradation using nano-enabled photocatalysts. J. Water Process Eng. 54, 103880. https://doi.org/10.1016/j.jwpe.2023.103880.
Sacco, O., Vaiano, V., Sannino, D., 2020. Main parameters influencing the design of photocatalytic reactors for wastewater treatment: a mini review. J. Chem. Technol. Biotechnol. 95 (10), 2608–2618. https://doi.org/10.1002/jctb.6488.
Sala-Garrido, R., Maziotis, A., Mocholi-Arce, M., Molinos-Senante, M., 2023. Assessing eco-efficiency of wastewater treatment plants: a cross-evaluation strategy. Sci. Total Environ. 900, 165839. https://doi.org/10.1016/j.scitotenv.2023.165839.
Salam, Md.A., Al-Amin, Md.Y., Salam, M.T., Pawar, J.S., Akhter, N., Rabaan, A.A., Alqumber, M.A.A., 2023. Antimicrobial resistance: a growing serious threat for global public health. Healthcare 11 (13), 1946. https://doi.org/10.3390/healthcare11131946.
Tra, V.T., Pham, V.T., Tran, T.-D., Tran, T.H., Tran, T.K., Nguyen, T.P.T., Nguyen, V.T., Dao, T.-V.-H., Tran, P.-Y.-N., Le, V.-G., Tran, C.-S., 2023. Enhance diclofenac removal in wastewater by photocatalyst process combination with hydrogen peroxide. Case Stud. Chem. Environ. Eng. 8, 100506. https://doi.org/10.1016/j.cscee.2023.100506.
Tufail, A., Price, W.E., Hai, F.I., 2020. A critical review on advanced oxidation processes for the removal of trace organic contaminants: a voyage from individual to integrated processes. Chemosphere 260, 127460. https://doi.org/10.1016/j.chemosphere.2020.127460.
Vallero, D.A., 2023. In *AccessScience*. Persistent, bioaccumulative, and toxic pollutants. McGraw Hill. https://doi.org/10.1036/1097-8542.500920.
Verlicchi, P., Galletti, A., Petrovic, M., Barceló, D., 2010. Hospital effluents as a source of emerging pollutants: An overview of micropollutants and sustainable treatment options. J. Hydrol. 389 (3–4), 416–428. https://doi.org/10.1016/j.jhydrol.2010.06.005.
Wang, D., Mueses, M.A., Márquez, J.A.C., Machuca-Martínez, F., Grčić, I., Peralta Muniz Moreira, R., Li Puma, G., 2021. Engineering and modeling perspectives on photocatalytic reactors for water treatment. Water Res. 202, 117421. https://doi.org/10.1016/J.WATRES.2021.117421.
Wang, N., Zheng, T., Zhang, G., Wang, P., 2016. A review on Fenton-like processes for organic wastewater treatment. J. Environ. Chem. Eng. 4 (1), 762–787. https://doi.org/10.1016/j.jece.2015.12.016.
Wei, S., Liu, X., Tao, Y., Wang, X., Lin, Z., Zhang, Y., Hu, Q., Wang, L., Qu, J., Zhang, Y., 2025. Strategy for enhanced soil lead passivation and mitigating lead toxicity to plants by biochar-based microbial agents. J. Hazard. Mater. 489, 137512. https://doi.org/10.1016/j.jhazmat.2025.137512.
Zenker, A., Cicero, M.R., Prestinaci, F., Bottoni, P., Carere, M., 2014. Bioaccumulation and biomagnification potential of pharmaceuticals with a focus to the aquatic environment. J. Environ. Manag. 133, 378–387. https://doi.org/10.1016/j.jenvman.2013.12.017.
Zhang, H., Xiong, X., Li, Y., Wang, L., Li, D., Feng, X., 2025. A multi-objective optimization approach for holistic planning of the water system in dry bulk ports: integrating life cycle assessment and life cycle costing. J. Water Process Eng. 72, 107456. https://doi.org/10.1016/j.jwpe.2025.107456.
Zhao, Y., Qiu, Y., Mamrol, N., Ren, L., Li, X., Shao, J., Yang, X., van der Bruggen, B., 2021. Membrane bioreactors for hospital wastewater treatment: recent advancements in membranes and processes. Front. Chem. Sci. Eng. 16, 634–660. https://doi.org/10.1007/s11705-021-2107-1.
Zhong, J., Jiang, H., Wang, Z., Yu, Z., Wang, L., Mueller, J.F., Guo, J., 2021. Efficient photocatalytic destruction of recalcitrant micropollutants using graphitic carbon nitride under simulated sunlight irradiation. Environ. Sci. Ecotechnol. 5, 100079. https://doi.org/10.1016/j.ese.2021.100079.